PERGAMON

Journal of Structural Geology 22 (2000) 1233–1246

JOURNAL OF STRUCTURAL GEOLOGY

www.elsevier.nl/locate/jstrugeo

Interaction and linkage of extension fractures and normal faults: examples from the rift zone of Iceland

Valerio Acocella [a,*], Agust Gudmundsson [b], Renato Funiciello [a]

[a] *Dip. Scienze Geologiche Università Roma Tre. Roma, Italy*
[b] *Geological Institute, University of Bergen, Bergen, Norway*

Received 9 June 1999; accepted 20 March 2000

Abstract

Field and photogeological studies were made of 90 zones of interacting fracture segments along the rift zone of Iceland. Each zone consists of a pair of extension fractures or a pair of normal faults, with lengths from metres to kilometres. These zones evolve from an underlapping stage, through an overlapping stage (the most common configuration) and, finally, to a linkage stage. Of all the zones, only 7% are underlapping, whereas 93% are overlapping, with hook-shaped fracture pairs. The length/width ratios of the overlapping zones have a mean value of 3.5. The preferred geometry of the overlapping zones depends upon the initial configuration of the interacting fractures (length, overstep) and the development of the interaction. In the overlapping zones, most fracture pairs show moderate shear (strike-slip) components, related to local variations in the extension (opening) directions. Vertical displacements on normal faults decrease as the overstep and length of overlapping zones increase; both, in turn, are proportional to the total lengths of the faults forming the pair. The geometrical and kinematic features of overlapping spreading centres at mid-ocean ridges show close similarities to those reported here. These similarities indicate that the architecture and evolution of overlapping zones are scale independent.

1. Introduction

Extension fractures and shear fractures are commonly composed of segments that show power-law length–size distributions (Segall and Pollard, 1983; Gudmundsson, 1987a; Scholz, 1990; Zhang et al., 1991; Cladouhos and Marrett, 1996; Cowie et al., 1996; Marrett et al., 1999). During the growth of a fracture, its segments interact mechanically and link up into gradually larger segments that, eventually, may form large structures (Macdonald and Fox, 1983; Pollard and Aydin, 1988; Dawers and Anders, 1995; Koukouvelas et al., 1999). The segment interaction and the overall fracture growth depends on various parameters, such as the remote differential stress field (Olson and Pollard, 1989), the initial configuration of the segments (Du and Aydin, 1991) and their propagation velocities (Olson, 1993).

Interactions between fracture segments in regimes of thrust faulting and strike-slip faulting have been studied in the field (Aydin and Nur, 1982; Aydin and Schultz, 1990; An, 1997), in experiments (An and Sammis, 1996; An, 1998; Basile and Brun, 1999; Schreurs et al., 1999) and by means of numerical models (Segall and Pollard, 1980; Cox and Scholz, 1988; Olson and Pollard, 1991; Lebel and Mountjoy, 1995). Many studies have also been made of the interactions between segments of extension fractures and between segments of normal faults, in continental areas (Gibbs, 1984; Ebinger, 1989; Faulds et al., 1990; Nelson et al., 1992; Childs et al., 1995; Clemson et al., 1997; McClay and Khalil, 1998; Ferrill et al., 1999) and at mid-oceanic ridges (Macdonald et al., 1984; Sempere and Macdonald, 1986; Macdonald et al., 1988; Grindlay and Fox, 1993; Taylor et al., 1994; Gudmundsson, 1995; Cowie, 1998; Macdonald, 1998).

* Corresponding author. Fax: +39-6-54888201.
E-mail address: acocella@uniroma3.it (V. Acocella).

0191-8141/00/$ - see front matter
PII: S0191-8141(00)00031-6

Numerical models (Pollard et al., 1982; Pollard and Aydin, 1984; Nicholson and Pollard, 1985; Gudmundsson et al., 1993; Willemse et al., 1996; Willemse, 1997; Maerten et al., 1999) and analogue models (Thomas and Pollard, 1993; Mauduit and Dauteuil, 1996; Acocella et al., 1999) have been used to study the mechanical interactions of fractures in extensional regimes. Theoretical results indicate that the geometry of interacting segments of normal faults or segments of extension fractures tends to be generally similar (Willemse, 1997), a common feature being partial overlap of hook-shaped fractures (e.g. Childs et al., 1995). For any two overlapping normal fault segments, the fault-displacement distribution in the overlap zone depends on the initial configuration of the faults (Maerten et al., 1999). These features may indicate a common mechanism that largely controls the mechanical interaction.

The first aim of this paper is to improve our understanding of the interaction between, and linking up of, segments of extension fractures and normal faults. For this purpose, we made field and photogeological studies of 47 zones between interacting segments of extension fractures and 43 zones between interacting segments of normal faults (metres–kilometres scale) in the rift zones of Iceland. A second aim is to use these data to develop a conceptual model on the evolution of the interaction between extension fractures and normal faults and to compare the model implications with data on overlapping spreading centres (hundreds–thousands of kilometres) at mid-ocean ridges.

2. Tectonic framework

The Icelandic part of the Mid-Atlantic Ridge contains two main volcanic zones: the East Volcanic Zone (EVZ), approximately 400 km long and 60 km wide, and the West Volcanic Zone (WVZ), which is a continuation of the Reykjanes Ridge and approximately 200 km long and 40 km wide. The EVZ is shifted by many tens of kilometres towards the east with regard to the ocean ridges north and south of Iceland, resulting in ocean-ridge discontinuities in the northern and southern parts of Iceland (Fig. 1). In North Iceland, the Tjornes Fracture Zone, a transform fault that is partly strike-slip and partly extensional, connects the Kolbeinsey Ridge with the EVZ (Young et al., 1985; Gudmundsson et al., 1993; Fjader et al., 1994; Langbacka and Gudmundsson, 1995; Rognvaldsson et al., 1998). In South Iceland, the segments of the volcanic zones partly overlap and give rise to the South Iceland Seismic Zone, SISZ (Gudmundsson and Brynjolfsson, 1993; Luxey et al., 1997; Bergerat et al., 1998). The SISZ consists of an area of active faulting, the primary seismogenic faults being NNE-trending dextral faults and ENE-trending sinistral faults (Bjarnason et al., 1993; Gudmundsson, 1995; Passerini et al., 1997;

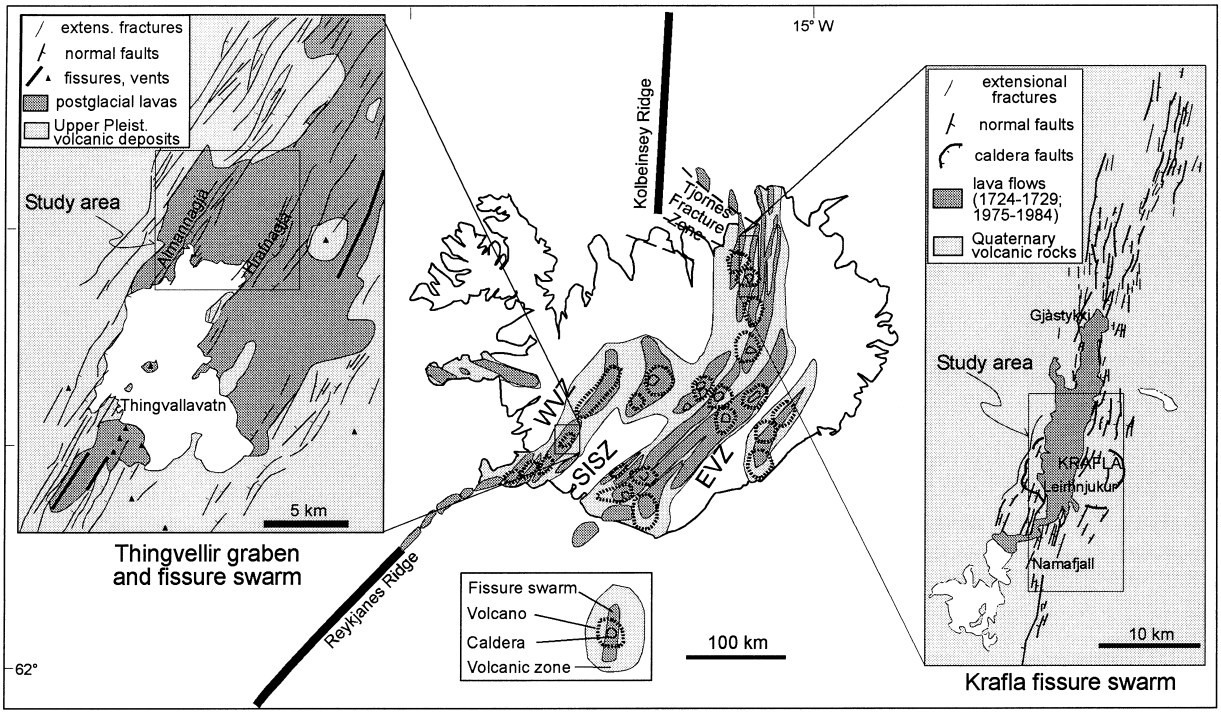

Fig. 1. Tectonic and volcanic features of the Icelandic part of the Mid-Atlantic Ridge. Insets show the main structural features of the investigated areas at Krafla and Thingvellir (modified from Opheim and Gudmundsson, 1989; Saemundsson, 1992; Johannesson and Saemundsson, 1998).

Bergerat et al., 1998). The SISZ also contains NE-trending normal faults that originated in the WVZ, but these are less active. The present-day stress field in the SISZ is partly related to the southwest propagation of the EVZ (Gudmundsson, 1995).

We studied 90 zones of interaction between overlapping segments of extension fractures and between overlapping segments of normal faults. Half the number of zones were measured in the Thingvellir graben, a part of the Thingvellir fissure swarm in the WVZ, the other half in the Krafla fissure swarm in the EVZ (Fig. 1). The Thingvellir fissure swarm marks the divergent plate boundary in Southwest Iceland. Its main structure, the 40-km-long and 5–7 km-wide Thingvellir graben, defined by the normal boundary faults Almannagja and Hrafnagja, dissects a 9000-year-old pahoehoe basaltic lava flow north of Lake Thingvellir (Gudmundsson, 1987b; Gudmundsson et al., 1992; Saemundsson, 1992).

The Krafla fissure swarm (Fig. 1), about 80 km long and 10 km wide, bisects the Krafla central volcano, a caldera (Tryggvason, 1986; Opheim and Gudmundsson, 1989) which was subject to a volcanotectonic episode in 1975–1984. The fissure swarm consists of vertical extension fractures, vertical normal faults and eruptive fissures.

We use the general term 'fracture' for all types of mechanical discontinuities or breaks in the host-rock, including the two main types of fractures discussed in this paper: extension fractures and normal faults. The term extension fracture is used when the separation is primarily by movement normal to the failure surface, but shear fracture (fault) when the separation is primarily by movement parallel to the failure surface. We infer that the extension fractures discussed in this paper are generally formed when the minimum principal compressive stress (considered positive) is negative so that they are true tension fractures. The fissure swarms of the rift zone in Iceland are thus named because they mostly contain fractures where the walls have moved apart, i.e. fissures (extension fractures and normal faults). The term crack is here regarded as synonymous with fracture as defined above. All these are traditional definitions in structural geology, but set forth here for convenience.

3. Geometrical features of interacting fractures

At Thingvellir the general trend of the fractures is northeast, whereas at Krafla it is north (Fig. 1). All the fractures are vertical at the surface, which in both fissures consists mostly of flat-lying pahoehoe lava flows. The surface is free of shear stress, so that vertical fractures at or near the surface must coincide with principal stress planes. There is no evidence that the fractures, either at Thingvellir or Krafla, are hydrofractures. It follows that the near-surface vertical parts of the fractures must be generated by absolute tension. Consequently, the extension fractures in these swarms are true tension fractures (formed when the minimum principal compressive stress is negative). Similarly, the uppermost parts of the normal faults are generated by absolute tensile stresses (Gudmundsson, 1987b). These stresses are generated in the rift zones as a consequence of the North American and the Eurasian plates being pulled apart at an average (spreading) rate of 1.8 cm/y (Gudmundsson, 2000).

The common stress field, similar trends and the same near-surface dips of the extension fractures and normal faults indicates a common origin. Thus, many of the normal faults develop from pre-existing extension fractures (Gudmundsson, 1987a; Opheim and Gudmundsson, 1989; Gudmundsson and Backstrom, 1991; Forslund and Gudmundsson, 1992; Gudmundsson, 1992; Angelier et al., 1997). The extension fractures, in turn, develop from columnar (cooling) joints

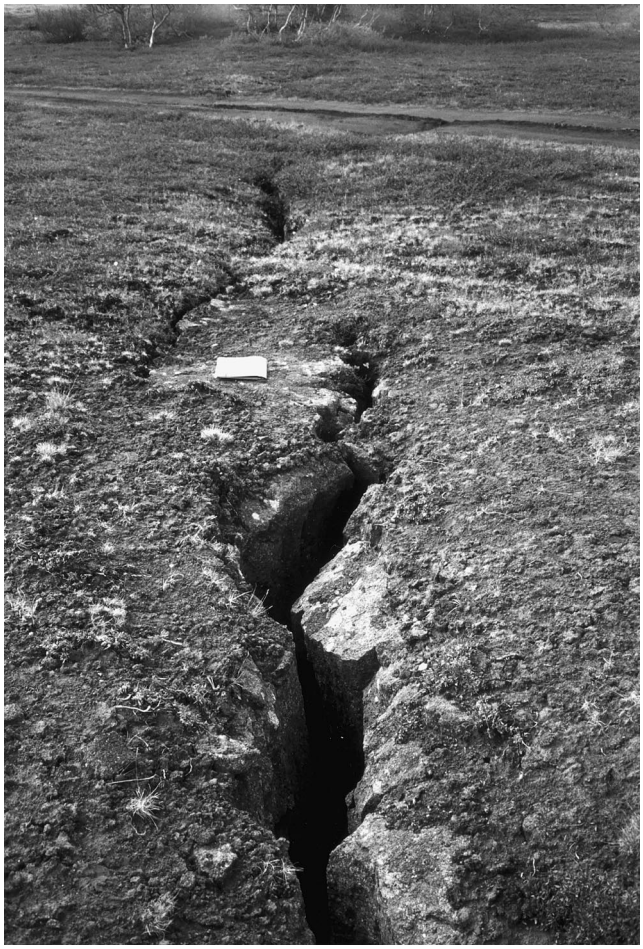

Fig. 2. Example of interacting opening-mode extensional fractures at Krafla. The extensional fractures interact forming an overlapping zone with hook-shaped paths.

in the basaltic lava flows. Some of the normal faults, particularly those that are closed at the surface, may also have developed directly from sets of columnar joints (Gudmundsson, 1992).

In our study, two segments (either of a pair of extension fractures or a pair of normal faults) are regarded as interacting if (a) the segments have an overlapping configuration and/or (b) the nearby tips of the segments become curved (in map view) while approaching each other. For nearly all such pairs, there develops an overlapping zone where the adjacent, propagating fractures become hook-shaped on approaching each other (Fig. 2). In only four of the 90 overlapping zones, all occurring in the Thingvellir fissure swarm, the crack–crack interactions lead to straight rather than hook-shaped overlapping fractures.

Our data indicate three main stages resulting from crack–crack interaction during the propagation of adjacent fracture tips (Fig. 3). In the first stage, the underlapping tips of the main fractures begin to curve slightly outwards from their earlier, straight pathways (Fig. 3a); around 7% of the overlapping zones are presently at this stage. In the next stage, the fractures develop a hook-shaped geometry (Figs. 2 and 3b); around 76% of the overlapping zones are currently at this stage. In the third stage, fracture segments link up and coalesce into a single, sinuous fracture (Fig. 3c); around 17% of the overlapping zones are presently at this stage. Thus, approximately 93% of the studied zones are at stages two or three and thus with overlapping segments, whereas 7% of the zones are with underlapping segments.

The main geometrical parameters of the overlapping zones, as defined in Fig. 4, were measured. As might be expected from the common origin of extension fractures and normal faults, their geometric and kinematic relationships are the same. This indicates that the mechanical behaviour of interacting extension fractures and interacting normal faults in Iceland is essentially uniform and depends on the same parameters.

An important measure of the overall architecture of overlapping zones is the aspect ratio $A = L/W$, where L is the length and W is the maximum width of the overlapping zones (Fig. 4). Around 88% of the aspect ratios are between 2 and 6, with a mean value of $A = 3.5$ (Fig. 5a). Clustering of the data around the mean value suggests that overlapping zones have certain pre-

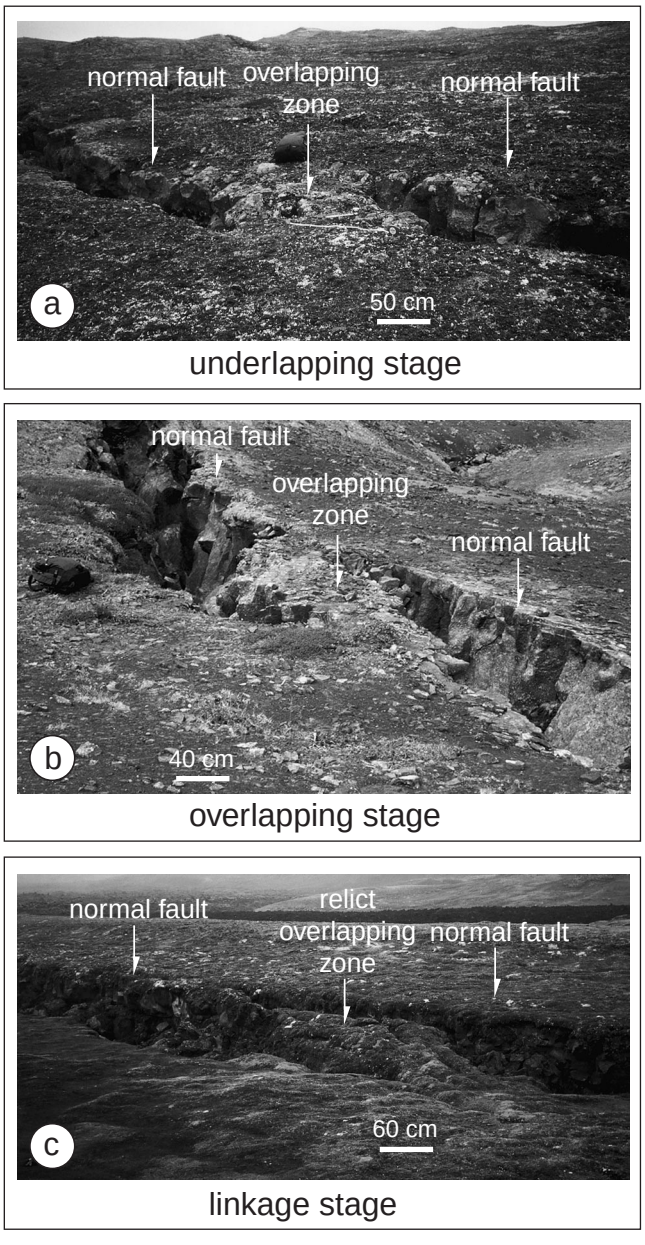

Fig. 3. The collected data allow us to distinguish schematically three stages of evolution of an interaction zone between small-scale (vertical displacement approximately 50 cm) normal faults (Krafla area). (a) Initial stage, characterised by an underlapping configuration of the fractures. (b) The propagation of the nearby tips of the normal faults promotes an overlapping configuration. (c) One of the normal faults propagates, linking with the other. The linkage stage is characterised by the development of a single continuous structure.

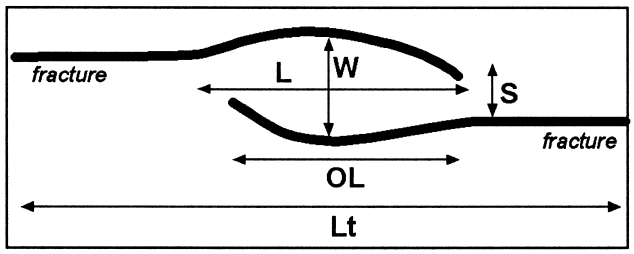

Fig. 4. Definition of the geometrical parameters associated with an overlapping zone. L_t = total length of both fractures; S = overstep between fractures; OL = overlap between fractures; L = maximum length, parallel to the direction of the fractures, of overlapping zone, limited by the points where the fractures start to curve; W = maximum width of overlapping zone, orthogonal to the direction of the fractures; L/W = aspect ratio of overlapping zone.

ferred geometric features. This conclusion is supported by the mean aspect ratio of the overlapping spreading centres on the East Pacific Rise being 3 (Sempere and Macdonald, 1986). A similar mean aspect ratio, 3.5, was obtained in field studies and in sand-box experiments on strike-slip fault segments (Aydin and Nur, 1982; Basile and Brun, 1999).

Some 12% of the zones have aspect ratios larger than 6, showing a slightly asymmetrical distribution (Fig. 5a). The skewing of the distribution towards the largest aspect ratios is because the width W (in the ratio $A = L/W$) increases with the overstep S (Fig. 5b). Interactions were also observed for initially collinear fractures (overstep $S = 0$). Then, however, W is smaller and A thus larger (Fig. 5b). Many of the high A values (Fig. 5a) are therefore related to fractures that were initially collinear.

The geometrical features of the overlapping zone depend also on the size (lengths) of the interacting fractures (Fig. 6). The data are scattered (especially for lower values), but all the diagrams show a positive correlation.

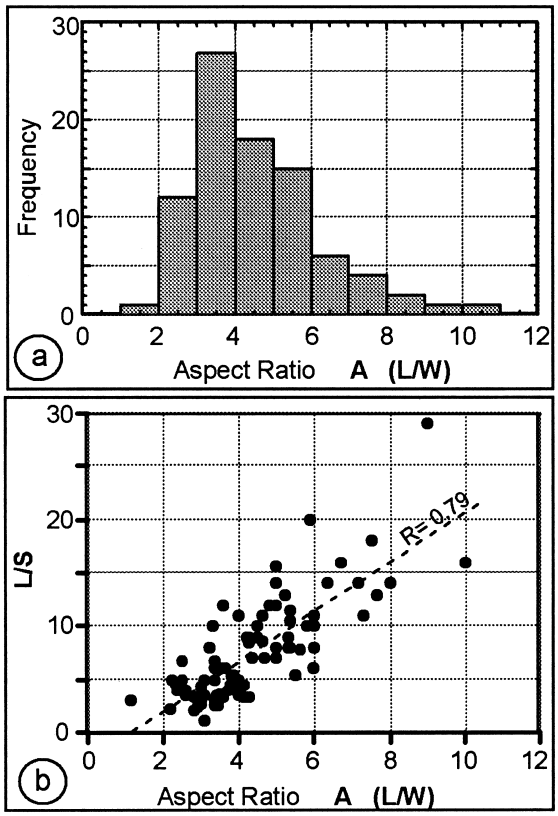

Fig. 5. (a) Aspect ratio (L/W) distribution of the overlapping zones between extensional fractures and normal faults at Krafla and Thingvellir. The mean value is $A = 3.5$. (b) Diagram showing the proportional relationship between the overstep S and the width W of overlapping zones, expressed as a function of the aspect ratio. Collinear fractures ($S = 0$) explain the presence of the asymmetric distribution in (a), characterised by 12% of zones with $A > 6$.

Comparison of the total length of the fracture pairs (L_t) and their oversteps S indicates that larger oversteps are associated with longer overlapping fractures (Fig. 6a). The lack of data showing interactions between fractures with a total length of the same order of magnitude as the overstep indicates that, for such a configuration, there is no interaction. Thus, for a given overstep, there is a critical minimum length for the fractures to interact and overlap; below this critical length no interaction and thus no overlapping occurs. From the slope of the linear best-fit curve, it follows that this minimum length has to be nearly 14 times the overstep between the fractures. This value may be significantly influenced by the host-rock properties and the local boundary conditions during fracture. Nevertheless, interactions between strike-slip fault segments in sand-box models yield similar minimum critical fault lengths (about 10 times their overstep) for linkage to occur (An, 1997). The lack of linkages for $L_t \gg S$ (Fig. 6b) indicates that no interaction occurs between fractures which are much longer than their oversteps.

The length L of an overlapping zone is proportional to the lengths of its overlapping fractures L_t (Fig. 6b). This suggests that two fractures start to 'feel' each other and interact when the along-strike distance (L) between their nearby ends decreases below a certain limit. The slope of the linear best fit curve indicates that, provided the fracture overstep is small (Fig. 6a), this distance is around 1/3 of the total fracture length L_t. This early stage of crack–crack interaction is commonly marked by the onset of the curved propagation of the fractures (Pollard and Aydin, 1984).

The overlap OL of the zones varies positively as the length of the fractures L_t (Fig. 6c); long fractures generate long overlapping zones (Fig. 6b) and thus large overlaps. OL depends also on the state of evolution or maturity of the overlapping zone. During an immature stage, the overlaps are short, so that $OL \ll L$ (Fig. 6d). Conversely, at a mature stage, overlap lengths are similar to zone lengths, so that $OL \approx L$ (Fig. 6d). This dependence of OL on zone maturity may partly explain the scatter of OL data (Fig. 6c and e).

For a broad range of scales, the length of the overlap OL between two segments is proportional to their overstep S (Fig. 6e). Although the data are quite scattered, the relationship indicates a clustering of OL/S ratios around a mean value of 4.9 (calculated from the individual ratios for each interaction zone). This relationship suggests that the architecture of natural overlapping zones develops within a limited range of proportions and that the overlapping configuration is primarily the result of a deterministic rather than a stochastic process. A similar relationship between overlaps and oversteps was obtained in a study of the linkage of natural normal faults (Huggins et al., 1995; Willemse, 1997)

and strike-slip faults (where the mean OL/S ratio = 4.7; Aydin and Schultz, 1990).

For a given overstep, the mean overlap OL (Fig. 6d and e) is presumably related to the maximum propagation energy of the interacting fracture pair (Pollard and Aydin, 1984; Aydin and Schultz, 1990). With a lower OL the growth of the overlapping zone is enhanced; With a higher OL its growth is inhibited. This explains why most (76%) of the studied interactions have reached a mature overlapping stage, whereas the great minority is in an underlapping stage (Fig. 3).

4. Kinematic features of interacting fractures

A systematic study was made of the asperities of the walls of the extensional fractures and normal faults. Most asperities are related to the columnar cooling joints in the lava flows and develop when these joints link up into extension fractures and normal faults (Forslund and Gudmundsson, 1992; Gudmundsson, 1992). Matching (in map-view) between the asperities of the walls of the fractures was used to evaluate the extension direction along the interacting fractures. Outside the overlapping zones there is good matching

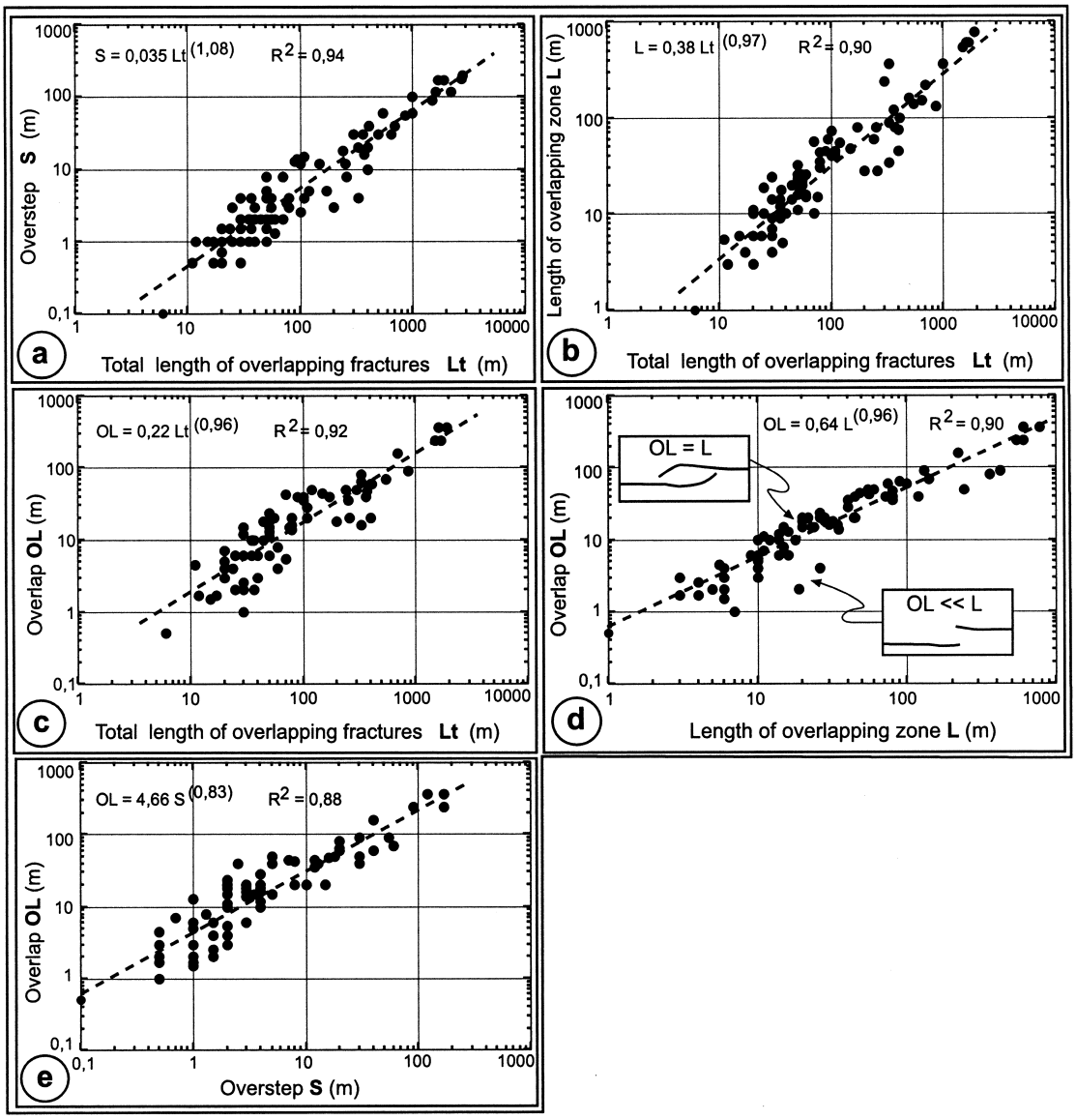

Fig. 6. (a) The overstep S between overlapping extensional fractures and normal faults at Krafla and Thingvellir is proportional to their total length L_t. (b) The length L of the overlap zone is proportional to the total length L_t of the fractures. (c) The overlap OL between overlapping fractures depends upon their total length L_t. (d) The overlap OL is proportional to the length L of the overlap zone. (e) The overstep S between interacting fractures is linearly proportional to the overlap OL for a broad range of scales, with a preferred OL/S ratio of 4.9. See text for further details.

between asperities of nearly all the fractures. Thus, the extension directions are orthogonal to the fracture trends, indicating a pure opening-mode extension. Conversely, in the overlapping zones, mismatch between the asperities of the fracture walls is common (Fig. 7), indicating components of strike-slip along the fractures.

The strike-slip components in the overlapping zone were measured using the angle β ($0^\circ < \beta < 90^\circ$) between the direction of extension and the direction orthogonal to the trend of the fracture (Fig. 8a); the direction orthogonal to the trend of the fracture varies along the segment and thus depends upon the part under consideration. For $\beta = 0^\circ$, the local direction of extension coincides with the direction orthogonal to the fracture: the fracture is thus generated by pure extension (pure opening). Conversely, if $\beta = 90^\circ$, the extension direction coincides with the trend of the fracture and the fracture is pure strike-slip. Positive values of β correspond to left-lateral, and negative values to right-lateral, horizontal shear on the fractures. All values and signs of β, and thus the sense of shear (left- or right-lateral) of the fractures in the overlap zone, were consistent with the direction of the fractures with regard to the extension direction.

The (absolute) values of the maximum horizontal shear β were measured in the field along parts of the hook-shaped fractures bordering the overlapping zone as well as along fractures inside the overlapping zone. The distribution of these values (Fig. 8b) indicates that for 82% of the shear along the fractures in the overlap zone β is between 20° and 50°. Horizontal shear with $\beta > 50^\circ$ is rare. These data show that moderate shear is common, but large shear is rare, on fractures in overlapping zones.

Fig. 7. Map view picture of an extensional fracture within an overlapping zone. The direction of the fracture is not orthogonal with regard to the extension direction (indicated by the lack of matching between asperities on fracture walls). The fracture thus shows a component of strike-slip displacement. Mixed-mode displacements such as this are commonly observed along fractures in overlapping zones.

The inferred direction of extension of fractures in an overlapping zone normally coincides with the 'regional' extension direction outside that zone. Nevertheless, in one or more parts of the fractures of around 75% of the overlapping zones, there are variations in the extension direction (Fig. 9). In these parts, the extension direction becomes locally perpendicular to the overlapping curved fractures. Similar local deviations from the regional extension in overlap zones, indicated by rotation of stress trajectories (Fig. 9), occur in photoelastic experiments (Gudmundsson, 1993; Gudmundsson et al., 1993). Thus, the extension directions within the overlapping zones are presumably related to both local and regional stresses.

For most overlapping normal faults, the fault displacement gradually decreases into the overlapping zone. Such a decrease in displacement is a common feature in relay ramps, as described by Peacock and Sanderson (1996) and Wojtal (1996) and modelled by Willemse et al. (1996) and Maerten et al. (1999). To estimate the displacement decrease (δ), with reference to the mean throw of the normal faults outside the overlap zone (Fig. 10a), we use the following equation:

$$\delta = (D1 + D2)/2 - (d1 + d2) \quad (1)$$

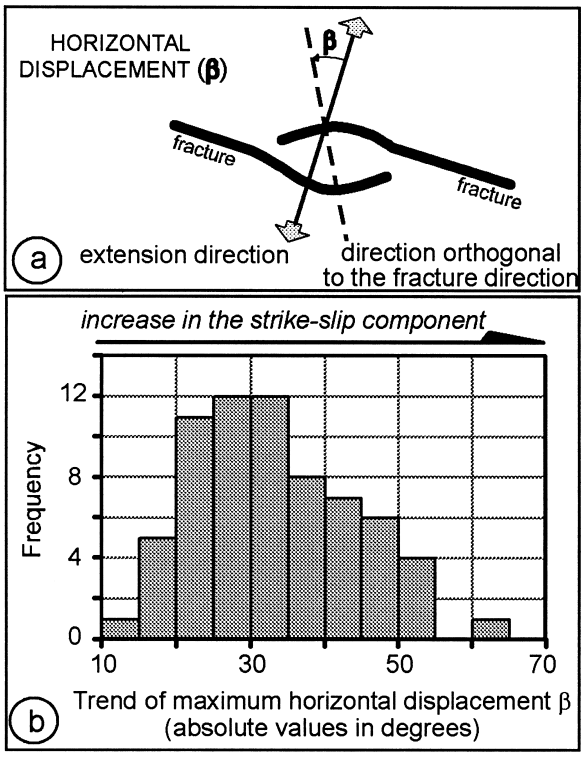

Fig. 8. (a) Definition of the component of strike-slip displacement β (angle between the extension direction and the orthogonal to the direction of the fracture) along overlapping extensional fractures and normal faults. (b) Distribution of the maximum values of β measured in overlapping zones between extensional fractures and normal faults at Krafla and Thingvellir. The mean value is $\beta = 30^\circ$.

where $D1$ and $D2$ are the mean displacements of the two interacting normal faults far from the overlapping zone and $d1$ and $d2$ are the minimum sums of displacements of the faults observed along a cross-section, perpendicular to the main fractures, in the overlapping zone (Fig. 10a). The displacement decrease, δ, is proportional to the total length of the normal faults L_t (Fig. 10b): longer faults show a greater displacement decrease. The displacement of a normal fault usually increases with fault length (Gudmundsson, 1992; Dawers and Anders, 1995). Thus, the δ/L_t linear relationship in Fig. 10(b) is partly a consequence of large normal faults correlating with large displacements and thus greater rates of displacement decrease in the overlap zone.

The displacement decrease δ in the overlap zone is also proportional to the overstep (S) between the adjacent normal faults (Fig. 10c). For negligible oversteps, the normal faults do not show a significant displacement decrease in the overlap zone. Thus, the two overlapping normal faults show a kinematic behaviour that approaches that of a single, larger, continuous normal fault. Numerical models have given similar results (Willemse et al., 1996). The relationship between δ and S (Fig. 10c) is related to the overstep increasing with the length of the fault (Figs. 6a and 10b): large faults have large oversteps and great rates of displacement decrease.

The relationship between the displacement decrease δ and OL (Fig. 10d) indicates that longer overlaps have greater δ. In turn, OL depends on the maturity and dimensions of the fault, resulting in a positive or negative correlation with δ. The positive correlation in Fig. 10(d), however, indicates that fault length has greater effects than maturity (cf. Cartwright et al., 1995) on the fault displacement variations.

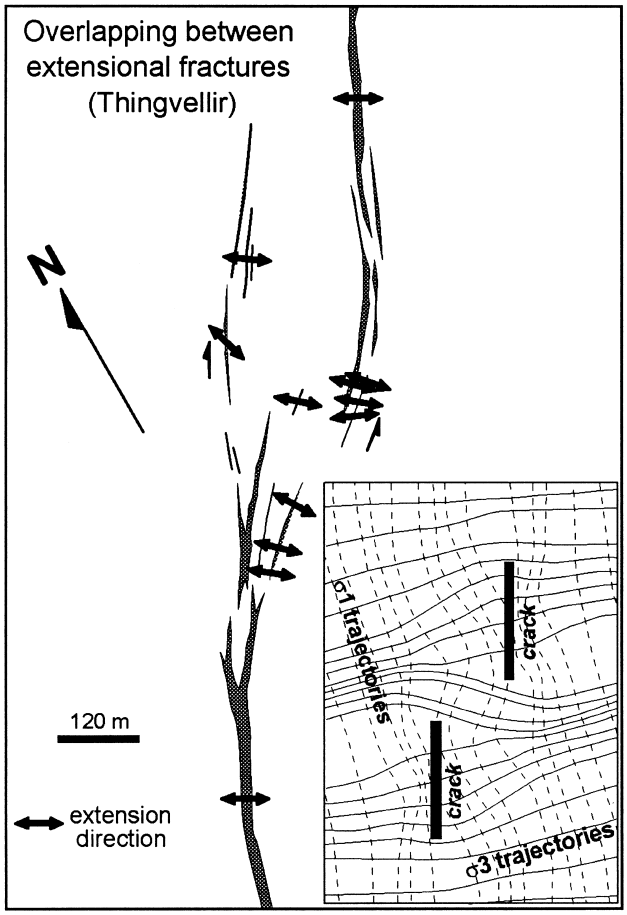

Fig. 9. Structural sketch of two interacting extensional fractures at Thingvellir, based on aerial photographs. The extension direction in the overlap zone, measured from the matching between wall asperities, is not parallel to the extension direction outside the overlap zone. This local extension direction is related to the rotation of the stress trajectories in the overlap zone (see inset, modified from Gudmundsson et al., 1993).

5. Discussion

5.1. Scaling implications

Overlapping zones are common in extensional domains (Macdonald et al., 1984; Peacock and Sanderson, 1991; Childs et al., 1995), the largest being the Overlapping Spreading Centres (OSC) of the mid-ocean ridges. In Fig. 11 we compare the geometrical features of the overlapping zones in Iceland with those of 15 OSC (Lonsdale, 1983; Lonsdale, 1985; Sempere and Macdonald, 1986; Haymon et al., 1991; Macdonald et al., 1992; Cormier and Macdonald, 1994; Lonsdale, 1994; Babcock et al., 1998). Our largest example of an overlapping zone, however, is the South Iceland Seismic Zone, SISZ (Gudmundsson and Brynjolfsson, 1993; Gudmundsson, 1995; Luxey et al., 1997; Bergerat et al., 1998).

The various geometrical ratios for the Icelandic overlapping zones are very similar to those of the mid-ocean ridges (Fig. 11). For example, OSC aspect ratio distribution closely matches that of the Icelandic data (Fig. 11a). The OSC and Icelandic data in Fig. 11(c–f) are consistent with a common best-fit curve and similar to the one in Fig. 6. Conversely, the OSC aspect ratio as a function of the L/S ratio (Fig. 11b) is slightly different from the Icelandic results, primarily because the OSC data have smaller L/S ratios. Thus, in comparison with small-scale overlapping zones in Iceland, overlapping ridges have larger oversteps.

As far as the kinematics of the overlapping zones are concerned, the best studied case of overlapping ridges is the SISZ. Its main features are NNE-trending dextral faults, ENE-trending sinistral faults and NE-trending normal faults. The overall sense of shear on these structures depends on the direction of the fractures with regard to the extension direction, which is

roughly E–W (Passerini et al., 1997; Bergerat et al., 1998; Gudmundsson, 2000). Inversions of focal mechanisms from the SISZ, however, suggest a local NW–SE extension superimposed on the regional E–W extension. Such a local extension may be induced by the shear stresses imposed by the rift-zone segments (Angelier et al., 1999). The clear kinematic similarities with our data suggest that this feature of the SISZ may constitute a large-scale analogue to the local perturbations in the extension direction of the overlapping zones observed in the fissure swarms.

The overall kinematic features of the SISZ thus show close analogies with the kinematic features of the collected data. The similarities between the small-scale data from the fissure swarms and the large-scale data from the overlapping spreading centres and from the SISZ suggest that the overall architecture of overlapping zones is scale invariant.

5.2. Evolutionary model

Our data suggest an evolutionary model on the formation, growth and coalescence of fractures along oceanic ridges. Extension fractures, commonly arranged en échelon, develop when the tensile stress across pre-existing columnar joints in the lava piles reaches the tensile strength simultaneously at many sites along the rift zone (Gudmundsson, 1987a). Thus, columnar joints constitute pre-existing weaknesses where the extensional fractures and, subsequently, normal faults start to nucleate (Gudmundsson, 1992).

These fractures form the segments of larger fractures. During along-strike propagation of the initial segments, they may eventually reach a length sufficient to interact with their neighbouring segments. Our data (Fig. 6a) suggest that the critical length of the segments for interaction to occur is approximately an order of magnitude larger than the oversteps between fractures; when this occurs, the distance L between the fractures is less than 1/3 of their length (Fig. 6b).

At the beginning of the interaction process, the fracture segments are characterised by an underlapping configuration (Fig. 12a). The propagation and linkage of the two underlapping ideal cracks are favoured until their tips pass each other and the cracks become overlapping (Pollard and Aydin, 1984; Willemse, 1997). The strong tendency for nearby tips of underlapping cracks to propagate may explain why underlapping segments are so rare (7% of our data; Fig. 3a).

An overlapping zone consists normally of adjacent, propagating fractures, with an overlapping configuration, that become hook-shaped on approaching each other (Fig. 12b). The hook-shape is a consequence of a local rotation of the extension direction (Fig. 9;

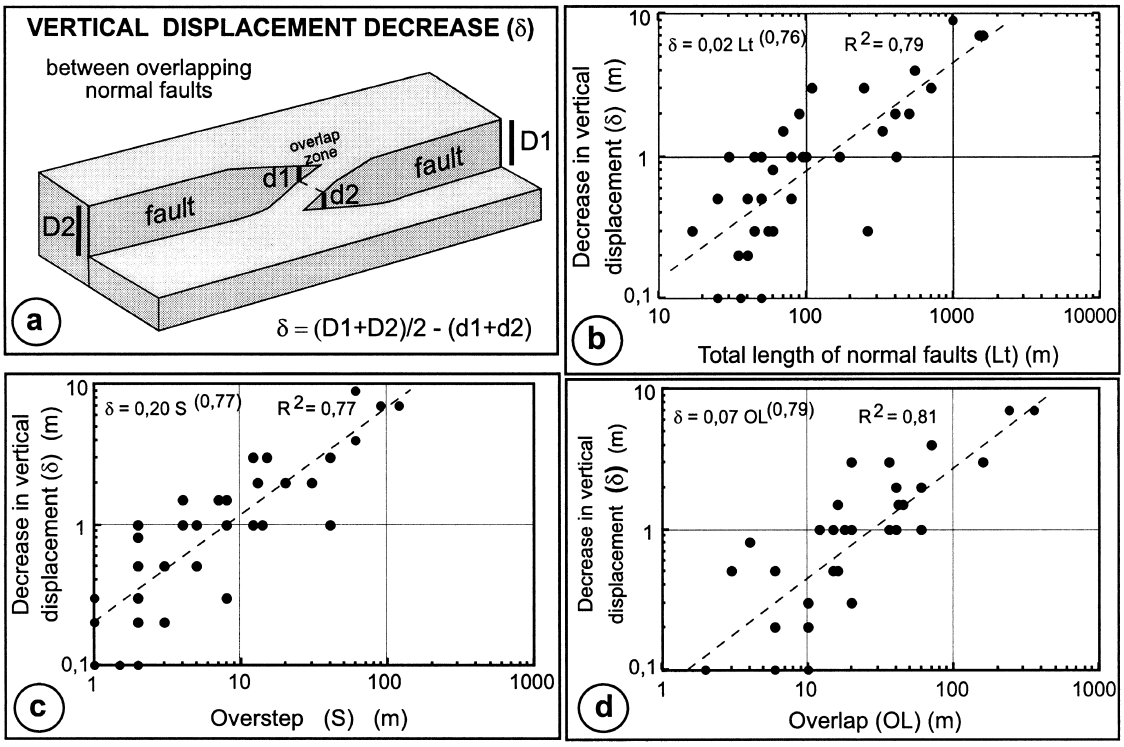

Fig. 10. (a) Definition of the decrease in vertical fault displacement δ as is commonly observed in overlapping zones between normal faults at Krafla and Thingvellir. The displacement decrease δ is proportional to the total length of the normal faults L_t (b), to the overstep S (c) and to the length of the overlap zone OL (d).

Gudmundsson, 1993; Gudmundsson et al., 1993). The degree of curvature of two hook-shaped overlapping fractures depends partly on the magnitude of the remote differential stress and partly on the fracture surface roughness (Olson and Pollard, 1989; Renshaw and Pollard, 1994). In our data, most fractures of the overlapping zones are curved; straight fractures occur only in few zones between normal fault pairs in the Thingvellir fissure swarm. The presence of straight (linear) overlapping structures may suggest great remote differential stress during normal fault propagation, the control of the asperities of the walls of the normal faults, or both (Olson and Pollard, 1989; Renshaw and Pollard, 1994).

The overlapping configuration of fractures constitutes the mature and most common stage of develop-

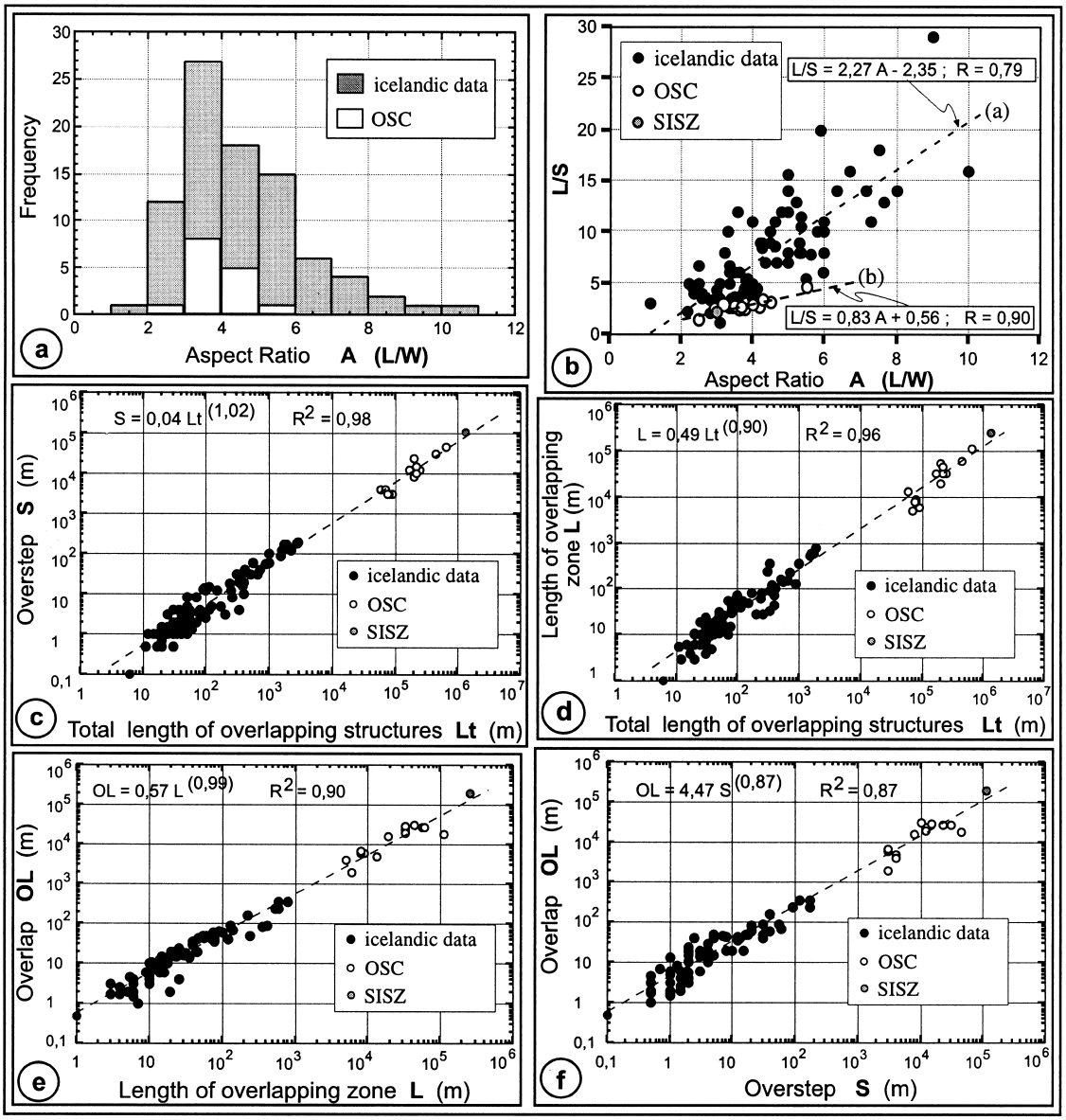

Fig. 11. Comparison between the collected geometrical data and the geometrical data relative to Overlapping Spreading Centres (OSC) as reported in previous works. (a) The aspect ratio distribution of the OSC and Icelandic overlapping zones is reported (see also Fig. 5a). (b) Variations of the aspect ratio (L/W) of the Icelandic overlapping zones (black dots, best fit curve 'a') and of the considered OSC (white dots, best fit curve 'b') as a function of the L/S ratio (see also Fig. 5b). Even though both data sets show equal aspect ratios, the OSC are characterised by lower L/S ratios. (c) Variation of the overstep S of OSC and Icelandic data as a function of the total length of the structures L_t. The best fit curve is relative to the whole data set (see also Fig. 6a). (d) Variation of the length of overlapping zone L of OSC and Icelandic data as a function of the total length of the structures L_t. The best fit curve is relative to the whole data set (see also Fig. 6b). (e) Variation of the overlap OL of OSC and Icelandic data as a function of the length L of the overlap zone. The best-fit curve is relative to the whole data set (see also Fig. 6d). (f) Variation of the overlap OL of OSC and Iceland data as a function of the overstep S. The best fit curve is relative to the whole data set (compare with Fig. 6e).

ment in the linkage process (Figs. 3b and 12b). During this stage, for a given fracture pair, the overlap OL progressively increases, approaching the length of the overlapping zone L (Fig. 6d). The overlapping zone develops a stable configuration with preferred geometrical features, which are responsible for the observed mean OL/S ratio of around 4.9 and a mean aspect ratio of around 3.5.

When the extensional segments eventually reach the linkage stage, one segment remains active, the other becomes abandoned. The result is a single, continuous, sinuous structure (Figs. 3c and 12c). When approaching this stage, the vertical displacement decrease of a normal fault in the overlapping zone becomes progressively reduced and the displacement gradually becomes nearly equal to that of a single, continuous normal fault.

Linkage may be reached more rapidly by fractures that have initial lengths longer (approximately one order of magnitude; Fig. 6a) than their initial spacing. By contrast, no overlapping zones have been observed where the fractures forming the pair are much longer (more than one order of magnitude; Fig. 6a) than their spacing. Apparently, these fractures were subject to a propagation force too great to maintain a stable overlapping zone. Transient geometries of this kind may occur in nature, but would rapidly lead to the propagation of the fractures into a single, large, sinuous structure. This stage thus depends on the time and the initial configuration of the fractures.

This model rests entirely on the Icelandic data, but yields similar results to models proposed for interacting large ridge segments, OSC (Macdonald and Fox, 1983; Macdonald et al., 1984; Sempere and Macdonald, 1986), suggesting scale independence. Our model also has close similarities with general models on the growth of normal faults (Peacock and Sanderson, 1991; Dawers and Anders, 1995; Walsh et al., 1999)

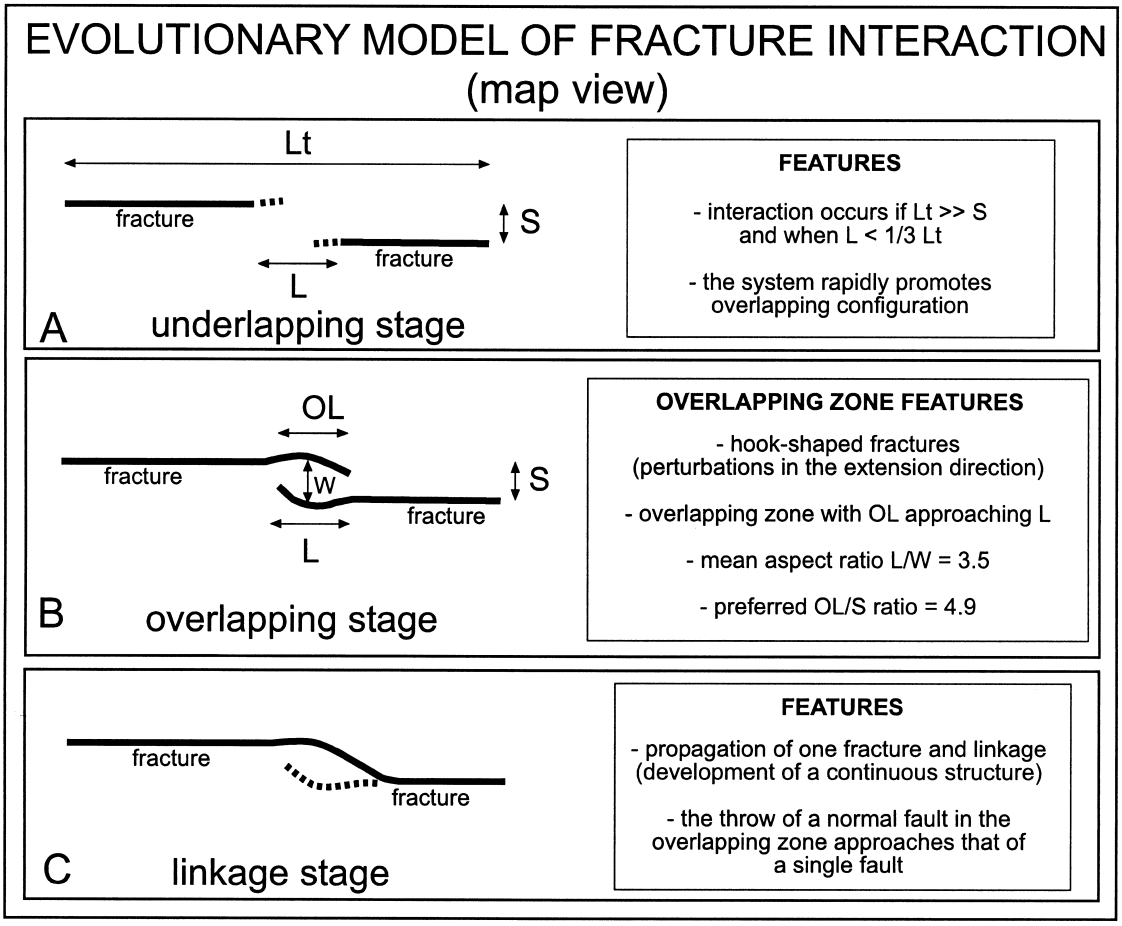

Fig. 12. Evolutionary model of interacting fractures along oceanic ridges. (a) A young overlapping zone is characterised by the interaction of two underlapping fractures with a length much longer than their overstep and a distance between the fractures less than 1/3 of their length. (b) The mature stage is characterised by the progressive overlap (OL approaching L) of hook-shaped fractures, defining an overlapping zone with a mean aspect ratio = 3.5 and OL/S ratio = 4.9. (c) The senile stage is constituted by the further propagation of one of the fractures and linkage with the other. This leads to the abandonment of the less-propagated segment and to the development of a single continuous structure. The displacement of the normal faults in the overlapping zone approaches that of a single fault.

and is consistent with the results from sand-box models of transfer zones in extensional domains (Acocella et al., 1999). The analogue models show échelon normal faults becoming hook-shaped in the transfer zone; strike-slip faults are present within the transfer zone with a sense of shear consistent with their trends with regard to the extension direction.

Furthermore, our results on overlapping zones between pairs of extension fractures and normal faults show close similarities to overlapping zones between pairs of strike-slip faults. A minimum length, at least one order of magnitude larger than the overstep, is required for the strike-slip faults to interact (An, 1997). Moreover, the overlapping zones between strike-slip segments have a mean aspect ratio of around 3.5 and an OL/S ratio of around 4.7 (Aydin and Nur, 1982; Aydin and Schultz, 1990), very similar to our results. The close correspondence between the architecture of overlapping zones associated with extension fractures, normal faults and strike-slip faults at various scales suggests that an essentially uniform mechanism controls the interaction process in all these overlapping zones.

Acknowledgements

The authors wish to thank O. Dauteuil and F. Salvini for helpful discussions, S. Birkir for hospitality at the Krafla Power Plant, and the reviewers M. Gross and J. Vermilye for helpful comments. This work was supported by Protezione Civile (Osservatorio Vesuviano) funds (to VA) and a grant (to AG) from the European Commission (contract ENV4-CT97-0536).

References

Acocella, V., Faccenna, C., Funiciello, R., Rossetti, F., 1999. Sandbox modelling of basement controlled transfer zones in extensional domains. Terranova 11, 149–156.

An, L., 1997. Maximum link distance between strike-slip faults: observations and constraints. Pure and Applied Geophysics 150, 19–36.

An, L.J., 1998. Development of fault discontinuities in shear experiments. Tectonophysics 293, 45–59.

An, L., Sammis, C.G., 1996. Development of strike-slip faults: shear experiments in granular materials and clay using a new technique. Journal of Structural Geology 18, 1061–1077.

Angelier, J., Bergerat, F., Dauteuil, O., Villemin, T., 1997. Effective tension–shear relationships in extensional fissure swarms, axial rift zone of northeastern Iceland. Journal of Structural Geology 19, 673–685.

Angelier, J., Bergerat, F., Rognvaldsson, S.Th., 1999. Using inversion of large population of earthquake focal mechanisms to derive the regional seismotectonic field: Iceland. Terranova abstract supplement EUG 10 11, 542.

Aydin, A., Nur, A., 1982. Evolution of pull-apart basins and their scale independence. Tectonics 1, 91–105.

Aydin, A., Schultz, A., 1990. Effect of mechanical interaction on the development of strike-slip faults within échelon patterns. Journal of Structural Geology 12, 123–129.

Babcock, J.M., Harding, A.J., Kent, G.M., Orcutt, J.A., 1998. An examination of along-axis variation of magma chamber width and crustal structure on the East Pacific Rise between 13°30′N and 12°20′N. Journal of Geophysical Research 103, 30451–30467.

Basile, C., Brun, J.P., 1999. Transtensional faulting patterns ranging from pull-apart basins to transform continental margins: an experimental investigation. Journal of Structural Geology 21, 23–37.

Bergerat, F., Gudmundsson, A., Angelier, J., Rognvaldsson, S.Th., 1998. Seismotectonics of the central part of the South Iceland Seismic Zone. Tectonophysics 298, 319–335.

Bjarnason, I.T., Cowie, P., Anders, M.H., Seeber, L., Scholz, C.H., 1993. The 1912 Iceland earthquake rupture: growth and development of a nascent transform system. Bulletin of the Seismological Society of America 83, 416–435.

Cartwright, J.A., Trudgill, B.D., Mansfield, C.S., 1995. Fault growth by segment linkage: an explanation for scatter in maximum displacement and trace length data from the Canyonlands grabens of SE Utah. Journal of Structural Geology 17, 1319–1326.

Childs, C., Watterson, J., Walsh, J.J., 1995. Fault overlap zones within developing normal fault systems. Journal of the Geological Society of London 152, 535–549.

Cladouhos, T.T., Marrett, R., 1996. Are fault growth and linkage models consistent with power-law distributions of fault lengths? Journal of Structural Geology 18, 281–293.

Clemson, J., Cartwright, J., Booth, J., 1997. Structural segmentation and the influence of basement structure on the Namibian passive margin. Journal of the Geological Society of London 154, 477–482.

Cormier, M.H., Macdonald, K.C., 1994. East Pacific Rise 18°–19°S: asymmetric spreading and ridge reorientation by ultrafast migration of axial discontinuities. Journal of Geophysical Research 99, 543–564.

Cowie, P.A., Knipe, R.J., Main, I.G., 1996. Introduction to the special issue. Journal of Structural Geology 18, v–xi.

Cowie, P.A., 1998. Normal fault growth in three-dimensions in continental and oceanic crust. In: Buck, W.R., Delaney, P.T., Karson, J.A., Lagabrielle, Y. (Eds.), Faulting at Magmatism at Mid-Ocean Ridges, Geophysical Monograph, 106, pp. 325–348.

Cox, S.J.D., Scholz, C.H., 1988. On the formation and growth of faults: an experimental study. Journal of Structural Geology 10, 413–430.

Dawers, N.H., Anders, M.H., 1995. Displacement–length scaling and fault linkage. Journal of Structural Geology 17, 607–614.

Du, Y., Aydin, A., 1991. Interaction of multiple cracks and formation of échelon crack arrays. International Journal of Numerical and Analytical Methods in Geomechanics 15, 205–218.

Ebinger, C.J., 1989. Geometric and kinematic development of border faults and accommodation zones, Kivu–Rusizi Rift, Africa. Tectonics 8, 117–133.

Faulds, J.E., Geissman, J.W., Mawer, C.K., 1990. Structural development of a major extensional accommodation zone in the Basin and Range Province, northwestern Arizona and Southern Nevada; implications for kinematic models of continental extension. Geological Society of America Memoir 176, 37–76.

Ferrill, D.A., Stamatakos, J.A., Sims, D., 1999. Normal fault corrugation: implications for growth and seismicity of active normal faults. Journal of Structural Geology 21, 1027–1038.

Fjader, K., Gudmundsson, A., Forslund, T., 1994. Dikes, minor faults and mineral veins associated with a transform fault in North Iceland. Journal of Structural Geology 16, 109–119.

Forslund, T., Gudmundsson, A., 1992. Structure of Tertiary and Pleistocene normal faults in Iceland. Tectonics 11, 57–68.

Gibbs, A.D., 1984. Structural evolution of extensional basin margins. Journal of the Geological Society of London 141, 609–620.

Grindlay, N.R., Fox, P.J., 1993. Lithospheric stresses associated with nontransform offsets of the mid-Atlantic ridge: implications from a finite element analysis. Tectonics 12, 982–1003.

Gudmundsson, A., 1987a. Geometry, formation and development of tectonic fractures on the Reykjanes Peninsula, southwest Iceland. Tectonophysics 139, 295–308.

Gudmundsson, A., 1987b. Tectonics of the Thingvellir fissure swarm, Iceland. Journal of Structural Geology 9, 61–69.

Gudmundsson, A., 1992. Formation and growth of normal faults at the divergent plate boundary in Iceland. Terranova 4, 464–471.

Gudmundsson, A., 1993. On the structure and formation of fracture zones. Terranova 5, 215–224.

Gudmundsson, A., 1995. Ocean-ridge discontinuities in Iceland. Journal of the Geological Society of London 152, 1011–1015.

Gudmundsson, A., 2000. Dynamics of volcanic systems in Iceland: example of tectonism and volcanism at juxtaposed hot spot and mid-ocean ridge systems. Annual Review of Earth and Planetary Sciences 28, 107–140.

Gudmundsson, A., Backstrom, K., 1991. Structure and development of the Sveinagja graben, northeast Iceland. Tectonophysics 200, 111–125.

Gudmundsson, A., Bergerat, F., Angelier, J., Villemin, T., 1992. Extensional tectonics of southwest Iceland. Bulletin of the Geological Society of France 163, 561–570.

Gudmundsson, A., Brynjolfsson, S., 1993. Overlapping rift-zone segments and the evolution of the South Iceland Seismic Zone. Geophysical Research Letters 20, 1903–1906.

Gudmundsson, A., Brynjolfsson, S., Jonnsson, M.T., 1993. Structural analysis of a transform fault-rift zone junction in North Iceland. Tectonophysics 220, 205–221.

Haymon, R.M., Fornari, D.J., Edwards, M.H., Carbotte, S., Wright, D., Macdonald, K.C., 1991. Hydrothermal vent distribution along the East Pacific Rise crest (9°09′–54′N) and its relationship to magmatic and tectonic processes on fast-spreading mid-ocean ridges. Earth and Planetary Science Letters 104, 513–534.

Huggins, P., Watterson, J., Walsh, J.J., Childs, C., 1995. Relay zone geometry and displacement transfer between normal faults recorded in coal-mine plans. Journal of Structural Geology 17, 1741–1755.

Johannesson, H., Saemundsson, K., 1998. Geological Map of Iceland. Tectonics, Iceland Institute of Natural History, Reykjavik. Scale 1:500,000.

Koukouvelas, I.K., Asimakopoulos, M., Doutsos, T.T., 1999. Fractal characteristics of active normal faults: an example of the eastern Gulf of Corinth, Greece. Tectonophysics 308, 263–274.

Langbacka, B.O., Gudmundsson, A., 1995. Extensional tectonics in the vicinity of a transform fault in North Iceland. Tectonics 14, 294–306.

Lebel, D., Mountjoy, E.W., 1995. Numerical modelling of propagation and overlap of thrust faults, with application to the thrust-fold belt of central Alberta. Journal of Structural Geology 17, 631–646.

Lonsdale, P., 1983. Overlapping rift zones at the 5.5° offset of the East Pacific Rise. Journal of Geophysical Research 88, 9393–9406.

Lonsdale, P., 1985. Nontransform offsets of the Pacific–Cocos plate boundary and their traces on the rise flank. Geological Society of America Bulletin 96, 313–327.

Lonsdale, P., 1994. Geomorphology and structural segmentation of the crest of the southern (Pacific–Antarctic) East Pacific Rise. Journal of Geophysical Research 99, 4683–4702.

Luxey, P., Blondel, P., Parson, L.M., 1997. Tectonic significance of the South Iceland Seismic Zone. Journal of Geophysical Research 102, 17967–17980.

Macdonald, K.C., Fox, P.J., 1983. Overlapping spreading centres: new accretion geometry on the East Pacific Rise. Nature 302, 55–58.

Macdonald, K., Sempere, J.C., Fox, P.J., 1984. East Pacific rise from Siqueiros to Orozco fracture zones: along strike continuity of the neovolcanic zone and structure and evolution of overlapping spreading centers. Journal of Geophysical Research 89, 6049–6069.

Macdonald, K.C., Fox, P.J., Perram, L.J., Eisen, M.F., Haymon, R.M., Miller, S.P., Carbotte, M.H., Shor, A.N., 1988. A new view of the mid-ocean ridge from the behaviour of ridge-axis discontinuities. Nature 335, 217–224.

Macdonald, K.C., Fox, P.J., Miller, S., Carbotte, S., Edwards, M.H., Eisen, M., Fornari, D.J., Perram, L., Pockalny, R., Scheirer, D., Tighe, S., Weiland, C., Wilson, D., 1992. The East Pacific Rise and its flanks 8–18° N: history of segmentation, propagation and spreading direction based on SeaMarc II and Sea Beam studies. Marine Geophysical Researches 14, 299–344.

Macdonald, K.C., 1998. Linkages between faulting, volcanism, hydrothermal activity and segmentation on fast spreading centers. In: Buck, W.R., Delaney, P.T., Karson, J.A., Lagabrielle, Y. (Eds.), Faulting at Magmatism at Mid-Ocean Ridges, Geophysical Monograph, 106, pp. 27–58.

Maerten, L., Willemse, E.J.M., Pollard, D.D., Rawnsley, K., 1999. Slip distributions on intersecting normal faults. Journal of Structural Geology 21, 259–271.

Marrett, R., Ortega, O.J., Kelsey, C.M., 1999. Extent of power-law scaling for natural fractures in rock. Geology 27, 799–802.

Mauduit, T., Dauteuil, O., 1996. Small-scale models of oceanic transform zones. Journal of Geophysical Research 98, 12251–12265.

McClay, K., Khalil, S., 1998. Extensional hard linkages, eastern Gulf of Suez, Egypt. Geology 26, 563–566.

Nelson, R.A., Patton, T.L., Morley, C.K., 1992. Rift-segment interaction and its relation to hydrocarbon exploration in continental rift systems. American Association Petroleum Geologists Bulletin 76, 1153–1169.

Nicholson, R., Pollard, D.D., 1985. Dilation and linkage of échelon cracks. Journal of Structural Geology 7, 583–590.

Olson, J., 1993. Joint pattern development: effect of subcritical crack growth and mechanical crack interaction. Journal of Geophysical Research 101, 20195–20209.

Olson, J., Pollard, D.D., 1989. Inferring paleostresses from natural fracture patterns: a new method. Geology 17, 345–348.

Olson, J.E., Pollard, D.D., 1991. The initiation and growth of en échelon veins. Journal of Structural Geology 13, 595–608.

Opheim, J.A., Gudmundsson, A., 1989. Formation and geometry of fractures and related volcanism of the Krafla fissure swarm, Northeast Iceland. Geological Society of America Bulletin 101, 1608–1622.

Passerini, P., Marcucci, M., Sguazzoni, G., Pecchioni, E., 1997. Longitudinal strike-slip faults in oceanic rifting: a mesostructural study from western to southeastern Iceland. Tectonophysics 269, 65–89.

Peacock, D.C., Sanderson, D.J., 1991. Displacement, segment linkage and relay ramps in normal fault zones. Journal of Structural Geology 13, 721–733.

Peacock, D.C., Sanderson, D.J., 1996. Effect of propagation rate on displacement variations along faults. Journal of Structural Geology 18, 311–320.

Pollard, D.D., Segall, P., Delaney, P.T., 1982. Formation and interpretation of dilatant échelon cracks. Geological Society of America Bulletin 93, 1291–1303.

Pollard, D.D., Aydin, A., 1984. Propagation and linkage of oceanic ridge segments. Journal of Geophysical Research 89, 10017–10028.

Pollard, D.D., Aydin, A., 1988. Progress in understanding jointing over the past century. Geological Society of America Bulletin 100, 1181–1204.

Renshaw, C.E., Pollard, D.D., 1994. Are large differential stresses required for straight fracture propagation paths? Journal of Structural Geology 16, 817–822.

Rognvaldsson, S.T., Gudmundsson, A., Slunga, R., 1998. Seismotectonic analysis of the Tjornes fracture zone, an active transform fault in North Iceland. Journal of Geophysical Research 103, 30117–30129.

Saemundsson, K., 1992. Geology of the Thingvallavatn area. Oikos 64, 40–68.

Scholz, C.H., 1990. The Mechanics of Earthquake Faulting. Cambridge University Press, Cambridge.

Schreurs, G., Hanni, R., Drayer, B., 1999. 4-D analysis of analogue models: examples of transfer zones in thrust belts. Terranova Abstract Supplement EUG 10 11, 610.

Segall, P., Pollard, D.D., 1980. Mechanics of discontinuous faults. Journal of Geophysical Research 85, 4337–4350.

Segall, P., Pollard, D.D., 1983. Joint formation in granitic rock of the Sierra Nevada. Geological Society of America Bulletin 94, 563–575.

Sempere, J.C., Macdonald, K., 1986. Overlapping spreading centers: implications from crack growth simulation by the displacement discontinuity method. Tectonics 5, 151–163.

Taylor, B., Crook, K., Sinton, J., 1994. Extensional transform zones and oblique spreading centers. Journal of Geophysical Research 99, 19707–19718.

Thomas, A.L., Pollard, D.D., 1993. The geometry of échelon fractures in rock: implications from laboratory and numerical experiments. Journal of Structural Geology 15, 323–334.

Tryggvason, E., 1986. Multiple magma reservoirs in a rift zone volcano: ground deformation and magma transport during the september 1984 eruption of Krafla, Iceland. Journal of Volcanology and Geothermal Research 28, 1–44.

Walsh, J.J., Watterson, J., Bailey, W.R., Childs, C., 1999. Fault relays, bends and branch-lines. Journal of Structural Geology 21, 1019–1026.

Willemse, E.J., 1997. Segmented normal faults: correspondence between three dimensional mechanical models and field data. Journal of Geophysical Research 102, 675–692.

Willemse, E.J., Pollard, D.D., Aydin, A., 1996. Three dimensional analyses of slip distributions on normal fault arrays with consequences for fault scaling. Journal of Structural Geology 18, 295–309.

Wojtal, S.F., 1996. Changes in fault displacement populations correlated to linkage between faults. Journal of Structural Geology 18, 265–279.

Young, K.D., Jancin, M., Voight, B., Orkan, N.I., 1985. Transform deformation of Tertiary rocks along the Tjornes fracture zone, North Central Iceland. Journal of Geophysical Research 90, 9986–10010.

Zhang, P., Slemmons, D.B., Mao, F., 1991. Geometric pattern, rupture termination and fault segmentation of the Dixie Valley–Pleasant Valley active normal fault system, Nevada, U.S.A. Journal of Structural Geology 13, 165–176.